NASA TECHNICAL MEMORANDUM

NASA TM X-71743

NASA TM X-71743

DYNAMIC CAPACITY AND SURFACE FATIGUE LIFE FOR SPUR AND HELICAL GEARS

by John J. Coy
U. S. Army Air Mobility Research and Development Laboratory
NASA - Lewis Research Center
Cleveland, Ohio 44135

and

Dennis P. Townsend and Erwin V. Zaretsky
Lewis Research Center
Cleveland, Ohio 44135

TECHNICAL PAPER to be presented at Joint Lubrication Conference cosponsored by the American Society of Lubrication Engineers and the American Society of Mechanical Engineers
Miami, Florida, October 21-23, 1975

DYNAMIC CAPACITY AND SURFACE FATIGUE LIFE FOR SPUR AND HELICAL GEARS

John J. Coy,* Dennis P. Townsend,** and Erwin V. Zaretsky**

Lewis Research Center
National Aeronautics and Space Administration
Cleveland, Ohio

ABSTRACT

A mathematical model for surface fatigue life of gear, pinion, or entire meshing gear train is given. The theory is based on the statistical approach used by Lundberg and Palmgren for rolling-element bearings. Also, equations are presented which give the dynamic capacity of the gear set. The dynamic capacity is the transmitted tangential load which gives a 90 percent probability of survival of the gear set for one million pinion revolutions.

The analytical results were compared with test data for a set of AISI 9310 spur gears operating at a maximum Hertz stress of 1.71×10^9 N/m^2 (248 000 psi) and 10 000 rpm. The theoretical life predictions were very good when material constants obtained from rolling-element bearing tests were used in the gear life model.

E-8273

NOMENCLATURE

b half width of Hertzian contact, m (in.)

c orthogonal shear stress exponent

E Young's modulus, N/m^2 (psi)

e Weibull's exponent

f face width of tooth, m (in.) (see fig. 1)

---

*Member, ASME; U.S. Army Air Mobility R&D Laboratory, Lewis Research Center.

**Member, ASME.

h	depth of critical stress exponent
K_1, K_2	constants of proportionality
L	pitting fatigue life in millions of revolutions
L_{GP}	gear life in terms of pinion rotations
L_1	life of a single pinion tooth
ℓ	involute profile arc length, m (in.)
ℓ_c	length of contact line, m (in.)
N	number of teeth
p_b	base pitch, m/tooth (in./tooth)
Q	normal tooth load, N (lb)
q	maximum contact stress, N/m^2 (psi)
r	pitch circle radius, m (in.)
r_a	addendum circle radius, m (in.)
r_b	base circle radius, m (in.)
S	probability of survival
V	volume, m^3 ($in.^3$)
W_t	transmitted tangential load, N (lb)
W_{tM}	dynamic capacity of the gear-pinion mesh, N (lb)
z_o	depth of occurrence of maximum orthogonal reversing shear stress, m (in.)
XYZ	right handed orthogonal coordinate systems
β_{Hl}	heavy load zone roll angle, rad
β_{Ll}	low load zone roll angle, rad
γ	tooth contact roll angle, rad
δ	precontact roll angle, rad

ζ length of zone of action, m (in.)

η millions of stress cycles

θ base circle roll angle, rad

σ Poisson's ratio

τ_o maximum subsurface orthogonal reversing shear stress, N/m^2 (psi)

ϕ_t transverse pressure angle, rad

ψ_b base helix angle, rad

Subscripts:

G gear

H high load

L low load

M mesh of pinion and gear

P pinion

1 reference to driving member

2 reference to driven member

INTRODUCTION

Gears used in power transmissions may fail in several different ways. Among those modes of failure are scoring of the gear tooth surface due to an inadequate lubricant film, tooth breakage caused by high bending stresses in the gear teeth, or surface fatigue pitting caused by repeated applications of high surface contact stress. The scoring type of failure of the gears may be eliminated by making changes in gear lubricant or gear tooth profiles [1 - 4]. Design methods for the avoidance of gear tooth breakage are based on the bending endurance limit of the gear material. Usually in these methods the gear tooth is analyzed as a cantilever beam with the addition of semi-empirical

service and geometry factors. If the maximum calculated bending stress is less than the endurance limit strength of the material then it is presumed that no tooth breakage will occur [5 - 7]. More exact calculations for the stress in bending have been made using finite element methods. The results are compared with AGMA and ISO standards on the strength of gear teeth in [8]. However, this work was done only for spur gear teeth. In 1960 Wellauer and Sierig presented a semi-empirical method for analyzing the helical gear tooth as a cantilevered plate, and the results were incorporated into a strength rating for helical gears [9, 10].

Current methods of design to resist surface fatigue are based on the concept of a surface fatigue endurance limit. The current method [11 - 13] of predicting gear tooth pitting failures is similar to that used for predicting tooth breakage. According to the method, the Hertzian contact stress is estimated and then modified with service condition and geometry factors to become the stress number. When the stress number is less than the surface fatigue endurance limit, it is assumed that the fatigue life is infinite. In [14] some gear life tests and roller life tests are reported. The authors state that it seems there is no pitting limit, but they are of the opinion that theoretically there is a surface endurance limit. Schilke [15] and Huffaker [16] believe that there is no endurance limit for surface fatigue. This belief has been the accepted criterion by the rolling element bearing industry since the publication of two important papers by Lundberg and Palmgren in 1947 and 1952 [17, 18].

Recently several authors have applied statistical methods for pre-

dicting gear life. In [19] a probabilistic method of deciding the allowable stress from a small amount of fatigue test results is presented. The method depends on the existence of a surface fatigue limit. Bodensieck [20] presented a stress-life-reliability system for rating gear life. His work is a nontraditional approach intended to give more precision to life and reliability predictions. Work has been done recently where the theory of Lundberg and Palmgren is applied to the problem of gear surface fatigue [21 - 23]. The Rumbarger surface fatigue life model [21], while a good approach in theory, may have some serious limitations as a design tool. In order to apply the model to life predictions several numerical evaluations of integrals must be carried out. In addition, there is some question regarding the accuracy of the equation pertaining to gear tooth profile incorporated into the model, and no full-scale gear tests were run to verify the accuracy of the model.

In [22] the experimental life obtained from fatigue testing of vacuum arc remelted (VAR) AISI 9310 spur gears was reported. Also the life theory for surface pitting of spur gears was derived. The theoretical and experimental lives were in good agreement. Also, experimental life studies have been conducted to determine the failure distribution of spur gears under various conditions [14 - 16, 22, 24], but unfortunately there is no similar experimental data for the case of helical gears.

In view of the aforementioned, it becomes the objective of the research reported herein to (1) provide a simplified theory for gear surface (pitting) fatigue failure from which calculations may readily

be made to provide life estimates of spur and helical gears and (2) to compare the analytical life prediction with experimental gear surface fatigue life data. The method of analysis is based on the rolling-element fatigue theory contained in [17]. Simplifications are incorporated into the failure theory for gears based on observations reported in [24] which reported that fatigue spalls on gears occurred in the region of the pitch point.

Fatigue Theory

The fatigue-life model proposed in 1947 by Lundberg [17] is the commonly accepted theory to determine the fatigue life of rolling-element bearings. The probability of survival is expressed as follows.

$$\log \frac{1}{S} \sim \frac{\tau_o^c n^e V}{z_o^h} \tag{1}$$

where

S probability of survival

V volume representation of the stress concentration or "stressed volume"

η millions of stress cycles

e Weibull slope

h,c material dependent exponents

τ_o critical stress

z_o depth of the critical stress

Unfortunately, no constant or proportionality was given by Lundberg and Palmgren for equation (1). However, by working back from a material constant given near the end of their paper the constant for use in equa-

tion (1) was determined [23]. Therefore, the equation for life with a 90-percent probability of survival may be written as follows.

$$L_1 = \left(\frac{K_1 z_o^h}{\tau_o^c V} \right)^{1/e} \tag{2}$$

where

$$K_1 = 1.430 \times 10^{95} \qquad \text{(SI units)}$$

$$= 3.583 \times 10^{56} \qquad \text{(English units)}$$

This constant was found to be valid for common bearing steel of 1950 vintage (AISI 52100) [14].

Based on life tests for roller bearings the accepted values for the exponents are

$$h = 2\frac{1}{3}$$

$$c = 10\frac{1}{3}$$

$$e = 1\frac{1}{2}$$

In the Lundberg and Palmgren theory, the load-life exponent for line contact is $p = (c - h + 1)/2e$. The Lundberg-Palmgren e and p are primary exponents which were obtained from bearing tests. The values of c and h were obtained from e and p and the results of tests made with a series of different sized bearings. The values of h and c are accepted for use in this paper, but the value of $e = 3$, which is based on gear tests reported in [15, 16, and 24] will be used in the calculation for gear life. Based on these values of h, c, and e a value of $p = 1.5$ results.

Much of the work by Lundberg and Palmgren was concerned with con-

necting the basic equation to common bearing geometry and operating parameters. In order for the theory to be directly useful and not involve cumbersome calculations, the same approach is used here for gears. In the next sections a rational way of treating the stress, stressed volume, and number of stress cycles for gear systems is presented. The derivations that follow deal mostly with helical geometry. By setting the helix angle to zero, the equations that follow apply to spur gears.

Maximum Hertzian Contact Stress

Current gear design practice is to estimate the stress at the pitch point of the teeth by assuming line contact between two cylinders whose radii depend on the curvature of the helical gear teeth at the pitch point. The unit loading on the contact line is estimated by assuming that the teeth are infinitely rigid and the load is distributed uniformly along the line of contact [25]. Another method of calculating load distributions by Matsunaga [26] is based on the assumption of a constant deflection of the teeth in mesh at any point on the line of contact. His calculations are made using an extension of the semi-empirical "moment-image" method of Wellauer and Sierig [9]. Matsunaga's calculations show a $2\frac{1}{2}$ to 1 variation in the theoretical unit loading across the contact line. However, the method of calculations neglects Hertzian and beam shearing deformations. He also noted from his gear tests that when pitting occurred, it was near the pitch line of the driving member. It is interesting to note that the highly loaded regions were near the lowest point of contact on the pinion. The author's [26] opinion was that scoring wear relieved the high stress in that area and, hence, the region near the pitch point became more highly stressed causing the resulting

pitch line pitting to occur. It is the authors' opinion that if a complete analysis considering bending, shear, and Hertzian deformations for the true helical gear mesh were possible, then the pitch point may be found to be the most highly loaded area. There are two reasons for this belief. One is that a fatigue spall requires both a high contact stress and a certain number of stress cycles for its formation. There is evidence that pitch line pitting can occur without prior scoring wear that alters the involute tooth form. The second reason is that the effect of tooth load sharing for spur gears is to cause the heaviest loads to occur near the pitch point. While it is more complicated to calculate this effect for helical gears, it is nevertheless probable that the same effect occurs. The main cause of the effect is the higher bending compliance of the gear tooth as the load nears the tip of the tooth.

In view of the foregoing observations, the classical approach to estimating the contact stress seems to be most appropriate at this time. Figure 1 shows the necessary geometry for estimating the Hertzian contact stress at the pitch point. Assuming line contact, the maximum Hertzian pressure is calculated by the formula [23]

$$q = \frac{2}{\pi b}\left(\frac{Q}{\ell_c}\right) \tag{3}$$

where ℓ_c is the length of the contact line and the load normal to the face of the tooth at the pitch point is given by

$$Q = \frac{W_t}{\cos \psi_b \cos \phi_t} \tag{4}$$

In the case of spur gears the length ℓ_c is the same as the face

width in contact. According to Hertz's theory for line contact, the equation for the semiwidth of the contact is [23]

$$b = \sqrt{\frac{8}{\pi \Sigma\rho}\left(\frac{Q}{\ell_c}\right)\left(\frac{1-\sigma^2}{E}\right)} \tag{5}$$

where

$$\Sigma\rho = \frac{\cos \psi_b}{\sin \phi_t}\left(\frac{1}{r_1} + \frac{1}{r_2}\right) \tag{6}$$

The depth to the critical stress and the maximum critical stress for line contact are given by

$$\tau_o = 0.25\ q \tag{7}$$

$$z_o = 0.5\ b \tag{8}$$

Contact Line Length

In figure 2 the zone of action is shown. Several lines of contact for mating pairs of teeth lie in the zone of action. The process that takes place can be imagined as a series of slanting lines (the contact lines) passing through a stationary viewing frame (the zone of action). The total length of the lines of contact ℓ_c may be calculated at each instant of time by graphical or analytical methods. For well designed gears the minimum length is said to be about 95 percent of the average total length of the contact lines [12].

$$\ell_c = 0.95\ \frac{\zeta f}{p_b \cos \psi_b} \tag{9}$$

Figure 3 shows the typical variation that occurs in the length of the contact lines for the helical gear. While it is recognized that the Hertz stress is not constant over the entire cycle of contact, it is felt that no large errors in approximation will be introduced since

the life varies inversely proportional to the load to the 1.5 power. This load-life exponent is based on the use of Lundberg and Palmgren's values of c and h ($c = 10\frac{1}{3}$, $h = 2\frac{1}{3}$) and on the Weibull slope $e = 3$ which is obtained from gear tests.

In the case of helical gears of low axial contact ratio, equation (9) becomes less accurate. Its use should be reserved for gears with axial contact ratio near two. For other cases ℓ_c should be calculated from the geometry in figure 2.

Stressed Volume

The volume representation which accounts for the size effect of the material in relation to the extent of the stress field was derived in [22] for spur gears. The following expression for stressed volume results

$$V = V_{spur} = \frac{3}{4} f z_o \ell \tag{10}$$

where ℓ is the involute length in the zone of single tooth contact. The product $f\ell$ is therefore a representation of the spur gear tooth surface area which is under contact stress. The factor 3/4 was introduced in [17]. This factor was used because a uniform stress distribution across the width of cylinder results when the semimajor axis of the contact ellipse is equal to $3\ell/4$.

In the case of helical gears the stressed volume is derived in [23] as

$$V = V_{helical} = \frac{3}{4} f z_o \ell \sec \psi_b \tag{11}$$

where ℓ denotes the length of involute in the transverse plane. The length ℓ in the case of spur gears was taken as the involute length over the region of a single-tooth pair in contact. In the case of

helical gears there is no equivalent length due to the gradually changing nature of the load sharing between the teeth. Therefore, several ways to treat the length may be possible depending on which assumption seems most reasonable for that situation. The simplest choice for ℓ would be to use the entire length of involute for which there is tooth action. This would be consistent with the assumption that the helical teeth are infinitely rigid and the only variation in tooth loading is caused by the changing length of the contact line as described in figure 3. An alternate assumption is that the length is calculated as for a spur gear using the transverse plane geometry. The second method is consistent with the assumption that the helical teeth can be modeled as spur teeth which are slightly displaced from one another along the helix angle as shown in figure 4. It is further assumed that there is no increase in stiffness of the elemental spur section caused by the adjacent spur sections. Therefore, these two cases are extremes which bracket the true load sharing ability of the helical gear teeth, and the results should provide reasonable lower and upper bounds to the statistical analysis of the life of a helical gear set.

Theoretical Gear Life and Dynamic Capacity

The load and geometry parameters of equations (3), (4), (5), (7), (8), and (11) are now combined with the basic life theory of equation (2). The result is an equation for the number of revolutions that a steel gear can endure with a 90-percent probability of survival of a given tooth.

$$L_1 = \left(\frac{K_2 \ell_c \cos \phi_t}{W_t} \right)^{3/2} (\cos \psi_b)^{11/6} (f\ell)^{-1/3} \Sigma\rho^{-35/18} \qquad (12)$$

K_2 = 132 000 when English units (lbf-in.) are used and 5.28×10^8 for SI units (N-m)

By definition, the dynamic capacity W_{tp} is the transmitted tangential load that may be carried for one million revolutions of the input drive,

$$W_{tp} = W_t L_1^{2/3} \tag{13}$$

The next step in the derivation is to develop the lives and dynamic capacities for the entire pinion, gear tooth, and entire gear, and finally for the system which is composed of the gear and pinion in mesh. The means of relating the lives and dynamic capacities of the pinion and gear to the life and dynamic capacity of the single pinion tooth is given by basic probability theory for independent events. For example, the probability of survival of the pinion is given by

$$S_p = S^{N_1} \tag{14}$$

Following this assumption, for 90-percent reliability, the lives of the pinion, gear, and mesh can be developed with the use of equations (1) and (14).

The resultant lives listed here are expressed in terms of millions of pinion rotations. Details of the derivation are in [22].

For the pinion,

$$L_p = N_1^{-1/3} L_1 \tag{15}$$

For a single gear tooth in terms of pinion rotations

$$L_{2P} = \left(\frac{N_2}{N_1}\right)^{4/3} L_1 \tag{16}$$

For the gear

$$L_{GP} = N_2^{-1/3} L_{2P} = N_2 N_1^{-4/3} L_1 \tag{17}$$

For the mesh of gear and pinion

$$L_M = \left\{ N_1 \left[1 + \left(\frac{N_1}{N_2} \right)^3 \right] \right\}^{-1/3} L_1 \tag{18}$$

The dynamic capacity of the gear tooth is given by

$$W_{tG} = \left(\frac{N_2}{N_1} \right)^{8/9} W_{tP} \tag{19}$$

For the gears in mesh the dynamic capacity is

$$W_{tM} = \left\{ N_1 \left[1 + \left(\frac{N_1}{N_2} \right)^3 \right] \right\}^{-2/9} W_{tP} \tag{20}$$

If equation (12) is used in (20) the final equation giving the dynamic capacity of the mesh may be written as

$$W_{tM} = K_2 \ell_c \cos \phi_t (\cos \psi_b)^{11/9} (\Sigma \rho)^{-35/27} \left[f \ell N_1 \left\{ 1 + \left(\frac{N_1}{N_2} \right)^3 \right\} \right]^{-2/9} \tag{21}$$

and if the actual transmitted tangential load is W_t then the corresponding life is given by

$$L = \left(\frac{W_{tM}}{W_t} \right)^{3/2} \tag{22}$$

Most of the terms in equation (21) may be calculated from information on standard gear dimensions. However, as was pointed out earlier, ℓ_c and ℓ, which are the length of the contact line and the length of the involute in the critically loaded region, respectively, are not as readily

determined. The approximate contact line length ℓ_c may be found directly from equation (9) or by an exact analysis. Also, as mentioned previously, there are two choices for the length of involute ℓ to be used in equation (21). The appendix gives some gear geometry that is useful in computing ℓ.

APPARATUS, SPECIMENS, AND PROCEDURE

Gear Test Apparatus

Spur gear fatigue tests were performed in the NASA Lewis Research Center's gear test apparatus (fig. 5). This test rig uses the four-square principle of applying the test gear load so that the input drive need only overcome the frictional losses in the system.

A schematic of the test rig is shown in figure 6. Oil pressure and leakage flow are supplied to the load vanes through a shaft seal. As the oil pressure is increased on the load vanes inside the slave gear, torque is applied to the shaft. This torque is transmitted through the test gears back to the slave gear, where an equal but opposite torque is maintained by the oil pressure. This torque on the test gears, which depends on the hydraulic pressure applied to the load vanes, loads the gear teeth to the desired stress level. The two identical test gears can be started under no load, and the load can be applied gradually, without changing the running track on the gear teeth.

Separate lubrication systems are provided for the test gears and the main gearbox. The two lubricant systems are separated at the gearbox shafts by pressurized labyrinth seals. Nitrogen was the seal gas. The test gear lubricant is filtered through a 5-micron nominal fiber-glass filter. The test lubricant can be heated electrically with an immersion-

heater. The skin temperature of the heater is controlled to prevent overheating the test lubricant.

A vibration transducer mounted on the gearbox is used to automatically shut off the test rig when a gear-surface fatigue occurs. The gearbox is also automatically shut off if there is a loss of oil flow to either the main gearbox or the test gears, if the test gear oil overheats, or if there is a loss of seal gas pressurization.

The test rig is belt driven and can be operated at several fixed speeds by changing pulleys. The operating speed for the tests reported herein was 10 000 rpm.

Test Lubricant

All tests were conducted with a single batch of super-refined naphthenic mineral oil lubricant having proprietary additives (anti-wear, antioxidant, and antifoam). The physical properties of this lubricant are summarized in table I. Five percent of an extreme pressure additive, designated Anglamol 81 (partial chemical analysis given in table II), was added to the lubricant. The lubricant flow rate was held constant at 800 cubic centimeters per minute, and lubrication was supplied to the inlet mesh of the gear set by jet lubrication. The lubricant inlet temperature was constant at 319±6 K ($115^{\circ}\pm10^{\circ}$ F), and the lubricant outlet temperature was nearly constant at 350±3 K ($170^{\circ}\pm5^{\circ}$ F). This outlet temperature was measured at the outlet of the test-gear cover. A nitrogen cover gas was used throughout the test as a baseline condition which allowed testing at the same conditions at much higher temperatures without oil degradation. This cover gas also reduced the effect of the oil additives on the gear surface boundary

lubrication by reducing the chemical reactivity of the additive-metal system by excluding oxygen [27].

Test Gears

Test gears were manufactured from vacuum arc remelted (VAR) AISI 9310 case carburized steel to an effective case depth of 1 mm (0.040 in.). The material chemical composition is given in table III and the heat treatment schedule is given in table IV. The nominal Rockwell C hardnesses of the case and core were 62 and 45, respectively. This material is a commonly used steel in gear manufacture.

Photomicrographs of the microstructure of the AISI 9310 are shown in figure 7. Figure 7(a) shows the high-carbon fine grained martensitic structure of the hardened case of the gear. Figure 7(b) shows the core region of the gear with its softer low-carbon refined austenitic grain structure.

Dimensions for the test gears are given in table V. All gears have a nominal surface finish on the tooth face of 0.406 micrometer (16 μin.) rms and a standard 20° involute tooth profile.

Test Procedure

The test gears were cleaned to remove the preservative and then assembled on the test rig. The test gears were run in an offset condition with a 0.30-centimeter (0.120 in.) tooth-surface overlap to give a load surface on the gear face of 0.28 centimeter (0.110 in.) of the 0.635-centimeter (0.250 in.) wide gear, thereby allowing for edge radius of the gear teeth. By testing both faces of the gears, a total of four fatigue tests could be run for each set of gears. All tests were run-in at a load of 1157 newtons per centimeter (661 lb/in.) for 1 hour. The

load was then increased to 5784 newtons per centimeter (3305 lb/in.) with a 1.71×10^{9} newton per square meter (248 000 psi) pitch-line Hertz stress. At the pitch-line load the tooth bending stress was 24.8×10^{8} newtons per square meter (35 100 psi) if plain bending is assumed. However, because there is an offset load there is an additional stress imposed on the tooth bending stress. Combining the bending and torsional moments gives a maximum stress of 26.7×10^{8} newtons per square meter (38 100 psi). This bending stress does not consider the effects of tip relief which will also increase the bending stress.

The test gears were operated at 10 000 rpm, which gave a pitchline velocity of 46.55 meters per second (9163 ft/min). Lubricant was supplied to the inlet mesh at 800 cubic centimeters per minute (0.21 gal/min) at 319±6 K ($115^{\circ}\pm10^{\circ}$ F). The tests were continued 24 hours a day until they were shut down automatically by the vibration-detection transducer located on the gearbox, adjacent to the test gears. The lubricant was circulated through a 5-micron fiber-glass filter to remove wear particles. A total of 3800 cubic centimeters (1 gal) of lubricant was used for each test and was discarded, along with the filter element, after each test. Inlet and outlet oil temperatures were continuously recorded on a strip-chart recorder.

The pitch-line elastohydrodynamic (EHD) film thickness was calculated by the method of Grubin [28]. It was assumed, for this film thickness calculation, that the gear temperature at the pitch line was equal to the outlet oil temperature and that the inlet oil temperature to the contact zone was equal to the gear temperature, even though the oil inlet temperature was considerably lower. It is probable that the gear surface

temperature could be even higher than the oil outlet temperature, especially at the end points of sliding contact. The EHD film thickness for these conditions was computed to be 0.65 micrometer (26 μin.), which gave a ratio of film thickness to composite surface roughness (h/σ) of 1.13.

RESULTS AND DISCUSSION

Gear fatigue tests were conducted with gears made from vacuum arc remelt (VAR) AISI 9310 steel. Test conditions were a load of 5784 newtons per centimeter (3305 lb/in.), which produced a maximum Hertz stress at the pitch line of 1.71×10^9 newtons per square meter (248 000 psi); a test speed of 10 000 rpm and a gear temperature of 350 K (170° F). A super-refined naphthenic mineral oil was the lubricant. Failure of the gears occurred due to surface fatigue pitting. Test results were statistically evaluated using the methods of [29]. The results of these tests are plotted on Weibull coordinates in figure 8. Weibull coordinates are the log-log of the reciprocal of the probability of survival graduated as the statistical percent of specimens failed (ordinate) against the log of time to failure or system life (abscissa). The experimental ten percent life or the life at a 90-percent probability of survival was 11.4 million revolutions or 19 hours of operation.

The theoretical ten percent life for this set of conditions was calculated using equation (17). The results of the calculation are listed in table VI. The exponents h and c and material constant K_2 are based on rolling-element bearing experience and the Weibull slope e is based on gear tests reported in [15, 16, and 24].

It should be remarked here that in the original work [17] the

Weibull slope e was assumed to be independent of the stress level and reliability level S. There is some evidence in [15] showing that the exponent e is dependent on the stress level. However, the value of e used above is a representative value at the stress level used in the gear tests performed at NASA.

Two cases are calculated in table VI. Case I was done using the length of involute in the heaviest load zone of single tooth contact giving a life of 54.9 hours. Case II was done using the entire involute length for which there is tooth contact giving a life of 33.2 hours.

The predicted life can be considered a reasonably good engineering approximation to the experimental life results. However, the theoretical prediction does not consider material and processing factors such as material type, melting practice, or heat treatment; nor does it consider environmental factors such as lubrication and temperature. All these factors are known to be extremely important in their effect on rolling-element bearing life [30]. There is no reason why these effects should be significantly different in determining gear life from those in determining gear life where pitting fatigue is the life-limiting criterion.

From [30] with a h/σ ratio of 1.13 the life adjustment factor due to lubrication effects is approximately 1/2. Therefore, the corrected values of life for cases I and II are 27 hours and 17 hours, respectively. As mentioned previously, the choice of involute length used gives lower and upper bounds for the predicted life. The theoretical failure distribution is plotted with the test data in figure 8. More test data obtained with gear specimens under various test conditions and different materials and lubricants are required to establish and/or

affirm the material constant K_2 and the exponents c, h, and e for gears. However, the results presented herein support the use of the statistical methods presented for predicting gear fatigue life with a standard involute profile.

SUMMARY OF RESULTS

An analytical model was developed to determine the fatigue life and dynamic capacity of spur and helical gears. The analytical results were compared with experimental gear life data obtained with a group of vacuum arc remelted (VAR) AISI 9310 spur gears. The test gears had a standard 20° involute profile and a 8.89-centimeter (3.5 in.) pitch diameter. Test conditions were a maximum Hertz stress of 1.71×10^9 newtons per square meter (248 000 psi), a speed of 10 000 rpm, and a temperature of 350 K (170° F). The lubricant was a super-refined naphthenic mineral oil with an additive package. The following results were obtained:

1. There was a good agreement between the predicted gear mesh life and the experimental life results.

2. The experimentally determined Weibull slope, e, for a sample of spur gears and the material constant K_2 and exponents h and c from roller-bearing life tests were used successfully to predict gear life. However, further experimental work is needed to give statistical significance to those exponents and the material constant.

3. The dynamic capacity of the spur or helical gear mesh is given by

$$W_{tM} = K_2 \ell_c \cos \phi_t (\cos \psi_b)^{11/9} (\Sigma\rho)^{-35/27} \left[f\ell N_1 \left\{ 1 + \left(\frac{N_1}{N_2} \right)^3 \right\} \right]^{-2/9} \qquad (23)$$

and the life corresponding to a particular transmitted load is given by

$$L = \left(\frac{W_{tM}}{W_t}\right)^{3/2} \tag{24}$$

APPENDIX - GEAR GEOMETRY NECESSARY FOR CALCULATING THE INVOLUTE LENGTH OF CONTACT ℓ

From figure 9 the differential length of involute profile in the transverse plane can be related to the roll angle of the pinion by the equation

$$d\ell = r_{b1}\theta_1 \, d\theta_1 \tag{A1}$$

After integration between any two angular positions of the pinion, the increment of involute length is

$$\ell = \frac{r_{b1}}{2}\left(\theta_{U1}^2 - \theta_{L1}^2\right) \tag{A2}$$

Figure 10 shows the load diagram for a spur gear with low contact ratio. A summary of the equations needed for calculation of the various angles shown on the abscissa of the load sharing diagram are derivable from the gear geometry. They are listed here for reference.

$$\delta_1 = \frac{(r_1 + r_2)\sin\phi_t - \sqrt{r_{a2}^2 - r_{b2}^2}}{r_{b1}} \tag{A3}$$

$$\beta_{L1} = \frac{\zeta - p_b}{r_{b1}} \tag{A4}$$

$$\beta_{H1} = \frac{2p_b - \zeta}{r_{b1}} \tag{A5}$$

where

$$\zeta = \sqrt{r_{a1}^2 - r_{b1}^2} + \sqrt{r_{a2}^2 - r_{b2}^2} - (r_1 + r_2)\sin\phi_t \tag{A6}$$

$$p_b = \frac{2\pi r_{b1}}{N_1} \tag{A7}$$

$$r_b = r \cos \phi_t \tag{A8}$$

If the length of involute for which only one pair of teeth in contact are wanted, use

$$\theta_{L1} = \delta_1 + \beta_{L1} \tag{A9}$$

$$\theta_{U1} = \theta_{L1} + \beta_{H1} \tag{A10}$$

If the entire length of the involute is wanted, then use

$$\theta_{L1} = \delta_1 \tag{A11}$$

$$\theta_{U1} = \theta_{L1} + 2\beta_{L1} + \beta_{H1} \tag{A12}$$

However, this set of equations was originally derived for the case of low contact ratio spur gears where $1 < \zeta/p_b < 2$. If the value of the transverse contact ratio is larger (i.e., $\zeta/p_b > 2$), then it is suggested that θ_{U1} be calculated with

$$\theta_{U1} = \delta_1 + \gamma_1 \tag{A13}$$

where γ_1 is the total pinion roll angle for which there is tooth contact.

$$\gamma_1 = \frac{\zeta}{r_{b1}} \tag{A14}$$

REFERENCES

1. Borsof, V. N., "One the Mechanism of Gear Lubrication," J. Basic Engr., Vol. 81, 1959, pp. 79-93.

2. Ishikawa, J., Hayashi, K, and Yokoyama, M., "Surface Temperature and Scoring Resistance of Heavy-Duty Gears," J. Eng. Ind., ASME Trans., vol. 96, 1974, pp. 385-390.

3. Blok, H., "Measurement of Surface Temperatures Under Extreme-Pressure Lubricating Conditions," Proc. of the Second World Petroleum Congress, Paris, Vol. 3, 1937, pp. 471-486.

4. Blok, H., "The Postulate About the Constancy of Scoring Temperature," Interdisciplinary Approach to the Lubrication of Concentrated Contacts, P. M. Ku, ed., NASA SP-237, 1970, pp. 153-248.

5. "Rating the Strength of Helical and Herringbone Gear Teeth," AGMA Paper No. 221.02, Aug. 1966.

6. "Rating the Strength of Spur Gear Teeth," AGMA Paper No. 220.02, Aug. Aug. 1966.

7. Seabrook, J. B., and Dudley, D. W., " Results of Fifteen-Year Program of Flexural Fatigue Testing of Gear Teeth," J. Engr. Ind., ASME Trans., Vol. 86, 1964, pp. 221-239.

8. Chabert, G., Dang Tran, T., and Mathis, R., "An Evaluation of Stresses and Deflections of Spur Gear Teeth Under Strain," J. Engr. Ind., ASME Trans., Vol. 96, 1974, pp. 85-93.

9. Wellauer, E. J., and Sierig, A., "Bending Strength of Gear Teeth by Cantilever Plate Theory," J. Engr. Ind., ASME Trans., Vol. 82, 1960, pp. 213-222.

10. Wellauer, E. J., "An Analysis of Factors Used for Strength Rating of Helical Gears," J. Eng. Ind., ASME Trans., Vol. 82, 1960, pp. 205-212.

11. "Surface Durability (Pitting) of Spur Gear Teeth," AGMA Paper No. 210.02, Jan. 1965.

12. "Surface Durability (Pitting) of Helical and Herringbone Gear Teeth," AGMA Paper No. 211.02, July 1965.

13. "Information Sheet for Surface Durability (Pitting) of Spur, Helical, Herringbone, and Bevel Gear Teeth," AGMA Paper No. 215.01, Sept. 1966.

14. Ishibashi, A., Ueno, T., and Tanaka, S., "Surface Durability of Spur Gears at Hertzian Stresses Over Shakedown Limit," J. Eng. Ind., ASME Trans., Vol. 96, 1974, pp. 359-372.

15. Schilke, W. E., "The Reliability Evaluation of Transmission Gears," SAE Paper No. 670725, Sept. 1967.

16. Huffaker, G. E., "Compressive Failures in Transmission Gearing," SAE Trans., Vol. 68, 1960, pp. 53-59.

17. Lundberg, G., and Palmgren, A., "Dynamic Capacity of Rolling Bearings," Ing. Vetanskops Akad., Handl., no. 196, 1947.

18. Lundberg, G. and Palmgren, A., "Dynamic Capacity of Roller Bearings," Ing. Vetenskaps Akad., Handl., no. 210, 1952.

19. Hayashi, K., Anno, Y., and Aiuchi, S., "Allowable Stresses in Gear Teeth Based on the Probability of Failure," ASME Paper No. 72-PTG-45, Oct. 1972.

20. Bodensieck, E. J., "A Stress-Life-Reliability Rating System for Gear and Rolling-Element Bearing Compressive Stress and Gear Root Bending Stress," AGMA Paper No. 229.19, Nov. 1974.

21. Rumbarger, J. H., and Leonard, L., "Derivation of a Fatigue Life Model for Gears," USAMRDL Technical Report 72-14, May 1972.

22. Coy, J. J., Townsend, D. P., and Zaretsky, E. V., "Analysis of Dynamic Capacity of Low-Contact-Ratio Spur Gears Using Lundberg-Palmgren Theory," proposed NASA Technical Note.

23. Coy, J. J., and Zaretsky, E. V., "Life Analysis of Helical Gear Sets Using Lundberg-Palmgren Theory," proposed NASA Technical Note.

24. Townsend, D. P., and Zaretsky, E. V., "A Life Study of AISI M-50 and Super-Nitralloy Spur Gears With and Without Tip Relief. J. Lubr. Tech., ASME Trans., Vol. 96, 1974, pp. 583-590.

25. Wellauer, E. J., " Helical and Herringbone Gear Tooth Durability - Derivation of Capacity and Rating Formulas," AGMA Paper No. 229.06, June 1962.

26. Matsunaga, T., "Influence of Profile Modification and Lubricant Viscosity on Scoring of Helical Gear," J. Eng. Ind., ASME Trans., Vol. 96, 1974, pp. 71-77.

27. Fein, R. S., and Kreuz, K. L., "Chemistry of Boundary Lubrication of Steel by Hydrocarbons," ASLE Trans., Vol. 8, 1965, pp. 29-38.

28. Dowson, D., and Higginson, G. R., Elasto-Hydrodynamic Lubrication, Pergamon Press, New York, 1966.

29. Johnson, L. G., The Statistical Treatment of Fatigue Experiments, Elsevier Publishing Co., New York, 1964.

30. Bamberger, E. N., et al., Life Adjustment Factors for Ball and Roller Bearings - An Engineering Design Guide, American Society of Mechanical Engineers, New York, 1971.

TABLE I. - PROPERTIES OF SUPERREFINED, NAPHTHENIC, MINERAL-OIL TEST LUBRICANT

Kinematic viscosity, cm^2/sec (cS), at	
266 K (20° F)	2812×10^{-2} (2812)
311 K (100° F)	73×10^{-2} (73)
372 K (210° F)	7.7×10^{-2} (7.7)
477 K (400° F)	1.6×10^{-2} (1.6)
Flash point, K (°F)	489 (420)
Autoignition temperature, K (°F)	664 (735)
Pour point, K (°F)	236 (-35)
Density at 289 K (60° F), g/cm^3	0.8899
Vapor pressure at 311 K (100° F), mm Hg (or torr)	0.01
Thermal conductivity at 311 K (100° F), J/(m)(sec)(K) (Btu/(hr)(ft)(°F))	0.04 (0.0725)
Specific heat at 311 K (100° F), J/(kg)(K) (Btu/(lb)(°F))	582 (0.450)

TABLE II. - PROPERTIES OF LUBRICANT ADDITIVE ANGLAMOL 81

Percent phosphorous by weight	0.66
Percent sulfur by weight	13.41
Specific gravity	0.982
Kinematic viscosity at 372 K (210° F), cm^2/sec (cS)	29.5×10^{-2} (29.5)

TABLE III. - CHEMICAL COMPOSITION OF VAR AISI 9310

GEAR MATERIAL BY PERCENT WEIGHT

Element	C	MN	SI	NI	CR	MO	CU	P&S
Weight percent	0.10	0.63	0.27	3.22	1.21	0.12	0.13	0.005

TABLE IV. - HEAT TREATMENT PROCESS FOR AISI 9310

Step	Process	Temperature, K (°F)	Time, hr
1	Carburize	1172 (1650)	8
2	Air cool to room temperature		
3	Copper plate all over		
4	Reheat	922 (1200)	2.5
5	Air cool to room temperature		
6	Austenitize	1117 (1550)	2.5
7	Oil quench		
8	Subzero cool	189 (-120)	3.5
9	Double temp	450 (350)	2 each
10	Finish grind		
11	Stress relieve	450 (350)	2

TABLE V. - SPUR GEAR DATA

[Gear tolerance per ASMA class 12.]

Number of teeth	28
Diametral pitch	8
Circular pitch, cm (in.)	0.9975 (0.3927)
Whole depth, cm (in.)	0.762 (0.300)
Addendum, cm (in.)	0.318 (0.125)
Chordal tooth thickness reference, cm (in.)	0.485 (0.191)
Pressure angle, deg	20
Pitch diameter, cm (in.)	8.890 (3.500)
Outside diameter, cm (in.)	9.525 (3.750)
Root fillet, cm (in.)	0.102 to 0.152 (0.04 to 0.06)
Measurement over pins, cm (in.)	9.603 to 9.630 (3.7807 to 3.7915)
Pin diameter, cm (in.)	0.549 (0.216)
Backlash reference, cm (in.)	0.0254 (0.010)
Tip relief, cm (in.)	0.001 to 0.0015 (0.0004 to 0.0006)

TABLE VI. - SAMPLE CALCULATION

Symbol	Description	Formula		Result	
ϕ_t	Transverse pressure angle, deg			20	
ψ_b	Base helix angle, deg			0	
P	Diametral pitch, teeth/cm (teeth/in.)			8	
a	Addendum			0.318 (0.125)	
N_1	Number of pinion teeth			28	
N_2	Number of gear teeth			28	
W_t	Transmitted tangential load, N (lb)			1617 (363)	
	Speed of pinion, rpm			10 000	
f	Face width in contact, cm (in.)			0.28 (0.11)	
r_1	Pinion pitch radius, cm (in.)	$N_1/2P$		4.445 (1.750)	
r_2	Gear pitch radius, cm (in.)	$N_2/2P$		4.445 (1.750)	
r_{a1}	Pinion addendum radius, cm (in.)	$r_1 + a$		4.763 (1.875)	
r_{a2}	Gear addendum radius, cm (in.)	$r_2 + a$		4.763 (1.875)	
r_{b1}	Pinion base circle radius, cm (in.)	$r_1 \cos \phi_t$		4.1769 (1.6445)	
r_{b2}	Gear base circle radius, cm (in.)	$r_2 \cos \phi_t$		4.1769 (1.6445)	
P_b	Base pitch, cm (in.)	$2\pi r_{b1}/N_1$		0.9373 (0.3690)	
ζ	Contact path length, cm (in.)	$\sqrt{r_{a1}^2 - r_{b1}^2} + \sqrt{r_{a2}^2 - r_{b2}^2} - (r_1 + r_2)\sin \phi_t$		1.5350 (0.6043)	
	Transverse contact ratio	ζ/p_b		1.64	
β_{H1}	Roll angle through heavy load zone, rad	$(2p_b - \zeta)/r_{b1}$		0.0813	
β_{L1}	Roll angle through light load zone, rad	$(\zeta - p_b)/r_{b1}$		0.1431	
δ_1	Precontact roll angle, rad	$\left[(r_1 + r_2)\sin \phi_t - \sqrt{r_{a2}^2 - r_{b2}^2}\right]/r_{b1}$		0.1802	
ℓ_c	Minimum face width in contact, cm (in.)	$\ell_c = f$		0.28 (0.11)	
$\Sigma\rho$	Curvature sum, cm^{-1} ($in.^{-1}$)	$(1/r_1 + 1/r_2)\cos \psi_b/\sin \phi_t$		1.316 (3.342)	
		Case I	Case II	Case I	Case II
θ_{L1}	Roll angle when load starts, rad	$\delta_1 + \beta_{L1}$	δ_1	0.3233	0.1802
θ_{U1}	Roll angle when load ends, rad	$\theta_{L1} + \beta_{H1}$	$\theta_{L1} + 2\beta_{L1} + \beta_{H1}$	0.4046	0.5477
ℓ	Length of stressed portion of involute, cm (in.)	$r_{b1}(\theta_{U1}^2 - \theta_{L1}^2)/2$		0.1237 (0.0487)	0.5587 (0.2200)
W_{tM}	Dynamic capacity of the mesh, N (lb)	$K_2 \ell_c \cos \phi_t (\cos \psi_b)^{11/9} (\Sigma\rho)^{-35/27} \left[f\ell N_1 \left\{1 + \left(\frac{N_1}{N_2}\right)^3\right\}\right]^{-2/9}$		16 600 (3732)	11 900 (2669)
L_M	Life of gear mesh, mr (hr)	$\left(\frac{W_{tM}}{W_t}\right)^{3/2}$		32.7 (54.9)	19.9 (33.2)

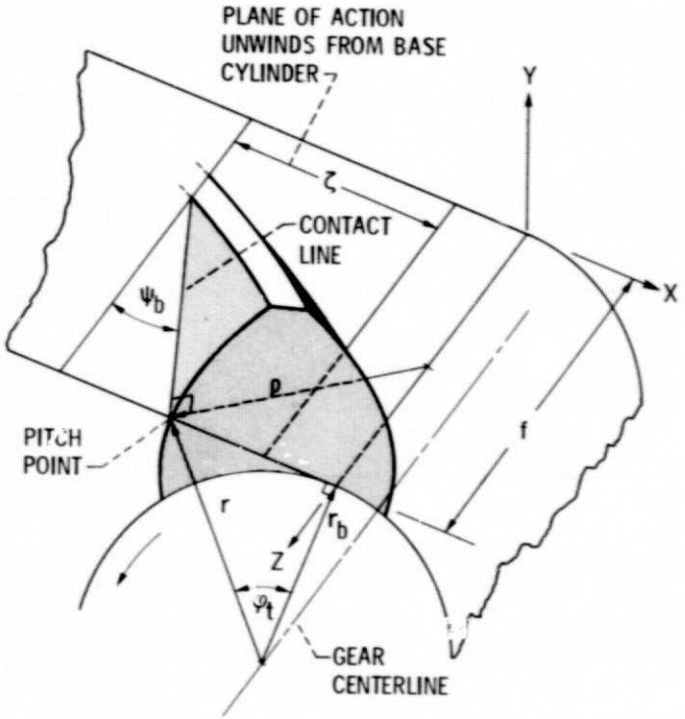

Figure 1. - Exaggerated view of helical gear tooth showing the base circle and plane of action. The contact line is the intersection of the tooth face and the plane of action. Contact between mating gear teeth occurs on the contact line.

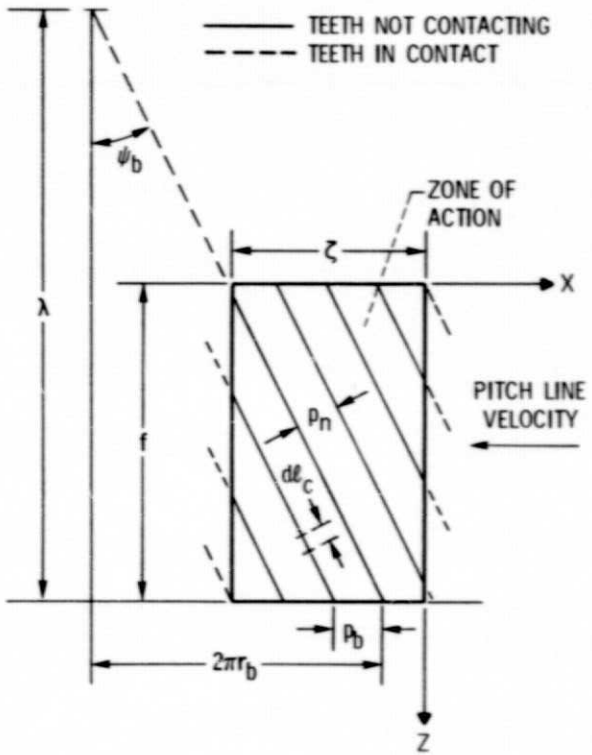

Figure 2. - The zone of action showing the lines of contact at the instant of initial tooth contact.

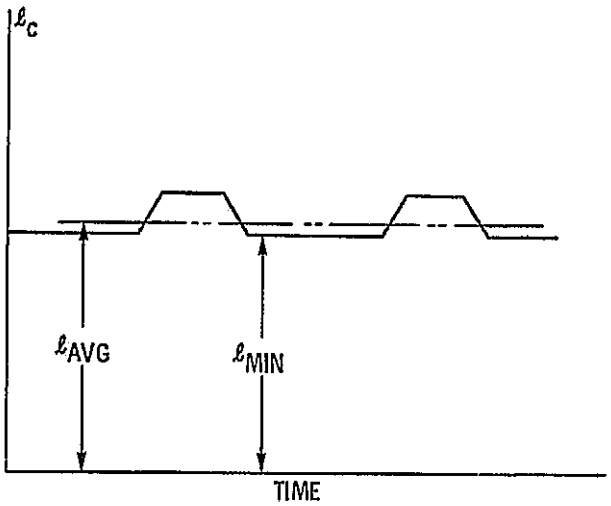

Figure 3. - Typical periodic variation in the total length of the contact lines in the helical gear mesh.

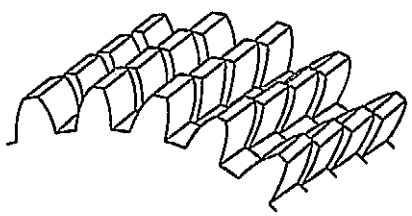

Figure 4. - Stepped spur gears. A helical gear results when there is a large number of very thin gear sections.

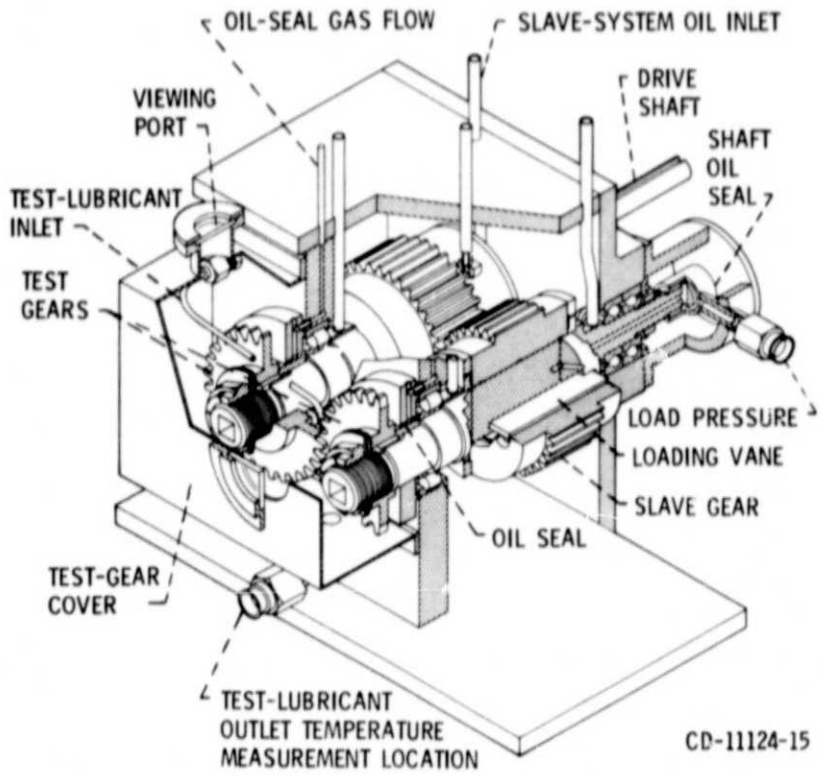

Figure 5. - NASA-Lewis Research Center's spur gear fatigue test apparatus.

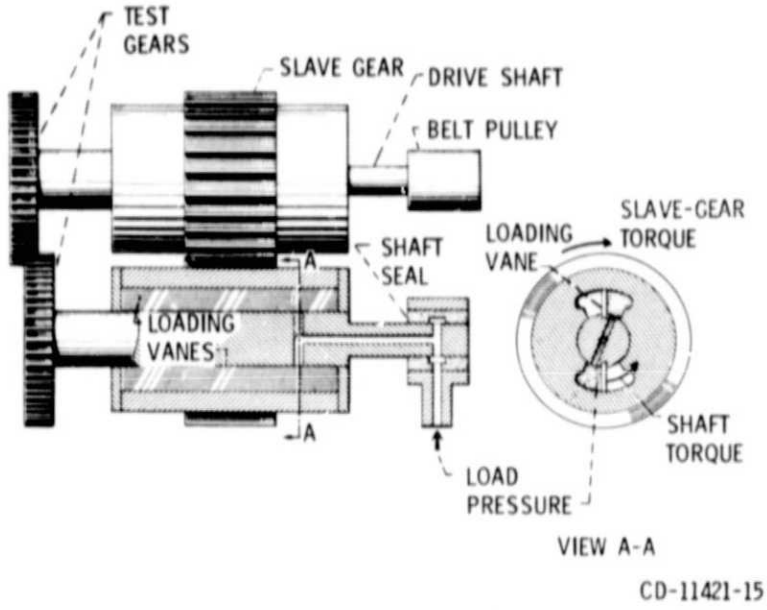

Figure 6. - Schematic diagram of spur gear fatigue apparatus.

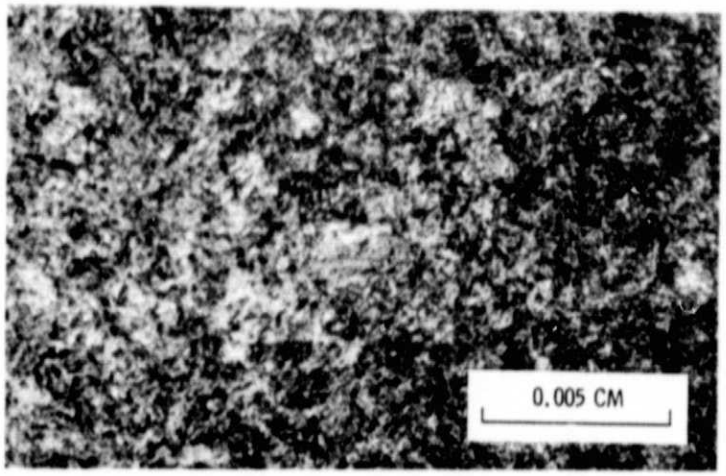

Figure 7(a). - Photomicrograph of the carburized and hardened case of the VAR AISI 9310 gear showing the high-carbon fine-grain martensitic structure.

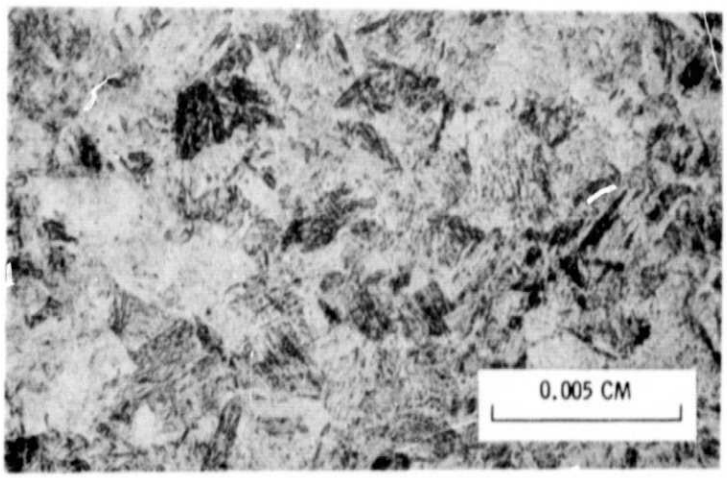

Figure 7(b). - Photomicrograph of the core structure of the VAR AISI 9310 gear showing the low-carbon refined austenitic grain size.

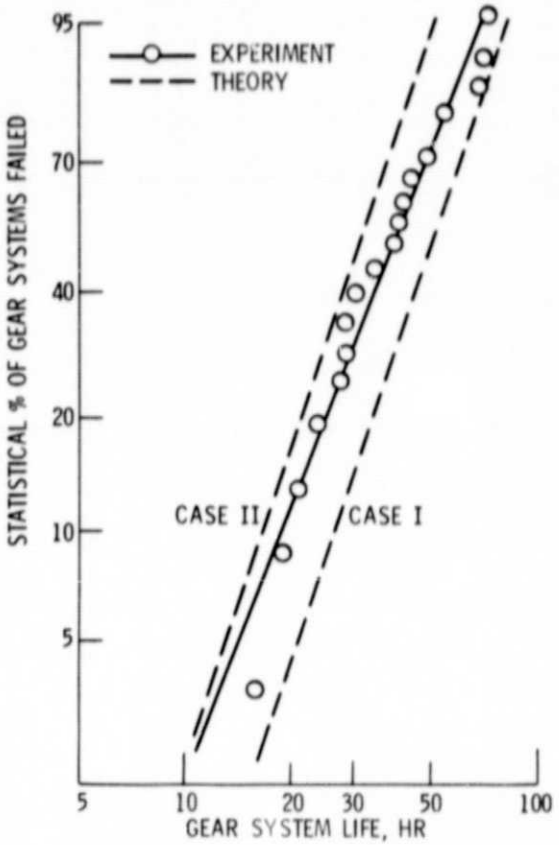

Figure 8. - Pitting fatigue lives of spur gear systems made of VAR AISI 9310. Maximum Hertz stress 1.71×10^9 N/m^2 (248 000 psi), speed 10 000 rpm, temperature 350 K (170^0 F), superrefined naphthenic mineral oil, Weibull slope 2.7.

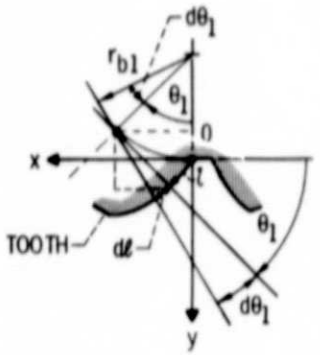

Figure 9. - Involute profile length.

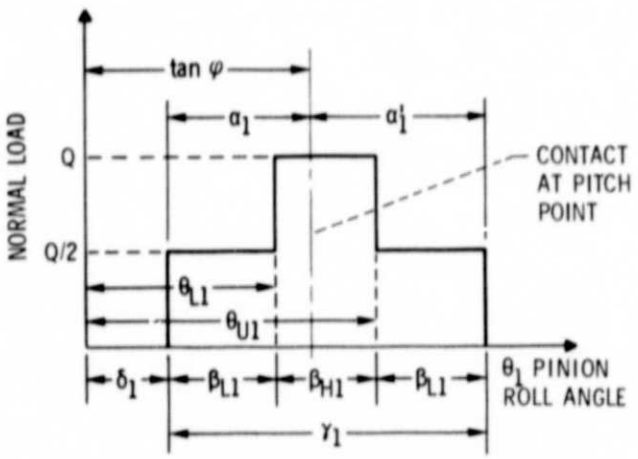

Figure 10. - Load sharing diagram. The load on a tooth for a low-contact ratio gear depends on the roll angle.